# Computational Prediction and Experimental Validation of the Unique Molecular Mode of Action of Scoulerine

**M. Moshari**
University of Alberta
**Q. Wang**
University of Alberta
**M. Michalak**
University of Alberta
**M. Klobukowski**
University of Alberta
**J. A. Tuszynski** ( jackt@ualberta.ca )
University of Alberta

**Research Article**

**Keywords:** Scoulerine, Protein Data Bank (PDB), binding sites, affinity values, microtubule stabilization, tubulin polymerization inhibition

**Posted Date:** May 13th, 2021

**DOI:** https://doi.org/10.21203/rs.3.rs-500519/v1

# Abstract

Scoulerine is a natural compound that is known to bind to tubulin and has anti-mitotic properties demonstrated in various cancer cells. Its molecular mode of action has not been precisely known. In this work we perform computational prediction and experimental validation of the mode of action of scoulerine. Based on the existing data in the Protein Data Bank (PDB) and using homology modeling we create human tubulin structures corresponding to both free tubulin dimers and tubulin in a microtubule. We then perform docking of the optimized structure of scoulerine and find the highest affinity binding sites located in both the free tubulin and in a microtubule. We conclude that binding in the vicinity of the colchicine binding site and near the laulimalide binding site are the most likely locations for scoulerine interacting with tubulin. Thermophoresis assays using scoulerine and tubulin in both free and polymerized form confirm these computational predictions. We conclude that scoulerine exhibits a unique property of a dual mode of action with both microtubule stabilization and tubulin polymerization inhibition, both of which have similar affinity values.


# Introduction

Natural products have played a dominant role in traditional medicine in over the previous centuries. In recent years, in spite of major advances in the computational drug discovery and total synthesis areas there has been a growing interest in using natural products for the development of anti-cancer therapeutics [1]. Some of these pharmaceutical agents have shown promising results in the prevention or treatment of cancer [2]. Scoulerine (also known as discretamine and aequaline) is a natural product isolated from Corydalis plants and belongs to one of the largest groups of natural compounds known as isoquinoline alkaloids [3]. Isoquinoline alkaloids are biogenetically derived from phenylalanine and tyrosine, having a basic structure of an isoquinoline or a tetrahydroisoquinoline ring in their scaffold [4]. Scoulerine molecule consists of two tetrahydroisoquinoline rings with two hydroxyls and two methoxyl functional groups (Figure 1). This molecule has shown a broad range of pharmacological properties such as antiemetic, antitussive, anti-bacterial, and anti-inflammatory activities [3]. It has also been demonstrated to have an anti-proliferative and pro-apoptotic function in cancer cells [5]. In addition, it is a precursor in the biosynthesis of noscapine, another natural compound with anti-mitotic properties that has been extensively tested in the cancer chemotherapy space [6–9].

Scoulerine inhibits b-site amyloid precursor protein cleaving enzyme 1 (BACE1), which is a very favourable target for Alzheimer's treatment [10]. It has been also recently reported that scoulerine exhibits effective antimitotic activity, which leads to microtubule disruption suggesting this molecule as a promising candidate for suppression of cancer cell growth [5].

Microtubules are ubiquitous filamentous structures found in the cytoskeleton of all eukaryotic cells. They polymerize from α and β tubulin heterodimers. Microtubules are dynamic polymers in kinetic equilibrium with the α, β tubulin heterodimers in solution which is achieved through polymerization and

depolymerization cycles [11]. Microtubules play a crucial role in the development and maintenance of cell shape. They are also importantly involved in mitosis and cellular movements [12]. Microtubules have been one of the most commonly considered targets for tubulin-targeting chemotherapeutic agents. The α, β tubulin heterodimers and microtubules have several different binding domains. Some of the well-studied inhibitors and their binding pockets are: the colchicine-binding domain, vinca-binding domain, laulimalide-binding domain, and taxol-binding domain, to list the most important few [11]. Most of the binding sites are not exclusive to primary inhibitors and can be targeted by other compounds. The mechanism of action of a large number of chemically diverse inhibitors of microtubules can be classified into two categories: they can act as either stabilizers or destabilizers. Microtubule-stabilizing agents stabilize the polymer by obstructing depolymerization and inducing the polymerization of tubulin [13]. Microtubule-destabilizing agents bind to the tubulin dimers and destabilize microtubules by halting polymerization of tubulin [14]. Despite the known effects of scoulerine on microtubules, a precise mechanism of action of this molecule is still unclear and further research is required [5].

The present study aims to address the mode of action of scoulerine by means of computational prediction studies. For this purpose, blind docking was used to predict binding pockets for scoulerine. An evaluation scheme based on binding affinities and root mean square deviation (RMSD) between the crystallographic and the docked ligand conformations leads to valuable initial information. For an expanded investigation into predicted binding sites for scoulerine, molecular dynamic (MD) simulations were used. The complex systems of scoulerine bound in the potential binding pockets were designed and analyzed by RMSD and clustering analysis. All of the above-mentioned steps were followed to predict the stability of the binding interactions and closeness of the inhibitor to the potential scoulerine binding sites.

# Materials And Methods

**3D structure preparation of the ligand.** The two-dimensional (2D) chemical structure of scoulerine was converted into a corresponding three-dimensional (3D) structure. The 3D scoulerine structure was first minimized and then fully optimized based on the RHF/ccpVDZ level of theory using the GAMESS-US software package (Version 2010-10-01) [31–34]. To investigate protonation of nitrogen in the scoulerine structure, the total energies of protonated and non-protonated scoulerine were calculated in the presence of hydronium and hydroxy ions in vacuum and water environments, respectively. The restricted Hartree-Fock method was used with the Dunning cc- pVDZ basis set for the above-mentioned calculations [31].

**Blind docking**. The optimized structure of scoulerine was blindly docked to the 1SA0 Protein Data Bank (PDB) structure of α and β tubulin *via* AutoDock4 software[16]. To do so, the maximum size of the grid box used was 126 × 126 × 126 $Å^3$, which then divided each of tubulin monomers into three parts and docking procedure was subsequently applied.

blind docking (BD) approach [3] was introduced previously

to search the entire surface of proteins for binding sites while

simultaneously optimizing the conformations of the peptides. The results of BD were regarded as “very encouraging” in a recent review [4].BD[5–7] and the recommended search parameters [8–12] have been used for solving various problems such as design of inhibitors [5], comparison of microtubule-stabilizing agents [7] and exploring substrate binding modes [8]. Because of the apparent success of the approach [4–12], we decided to perform further systematic tests on a set of 43 ligand–protein complexes which was previously used in a comprehensive study on the selectivity of binding of aromatic compounds [13]

The AutoDock [2]-based

blind docking (BD) approach [3] was introduced previously to search the entire surface of proteins for binding sites while simultaneously optimizing the conformations of the peptides. The results of BD were regarded as “very encouraging” in a recent review [4].BD[5–7] and the recommended search parameters [8–12] have been used for solving various problems such as design of inhibitors [5], comparison of microtubule-stabilizing agents [7] and exploring substrate binding modes [8]. Because of the apparent success of the approach [4–12], we decided to perform further systematic tests on a set of 43 ligand–protein complexes which was previously used in a comprehensive study on the selectivity of binding of aro-

matic compounds [13]

The AutoDock [2]-based

blind docking (BD) approach [3] was introduced previously

to search the entire surface of proteins for binding sites while

simultaneously optimizing the conformations of the peptides.

The results of BD were regarded as “very encouraging” in a

recent review [4].BD[5–7] and the recommended search

parameters [8–12] have been used for solving various prob-

lems such as design of inhibitors [5], comparison of microtu-

bule-stabilizing agents [7] and exploring substrate binding

modes [8]. Because of the apparent success of the approach

[4–12], we decided to perform further systematic tests on a

set of 43 ligand–protein complexes which was previously used

in a comprehensive study on the selectivity of binding of aro-

matic compounds [13]

The AutoDock [2]-based

blind docking (BD) approach [3] was introduced previously

to search the entire surface of proteins for binding sites while

simultaneously optimizing the conformations of the peptides.

The results of BD were regarded as “very encouraging” in a

recent review [4].BD[5–7] and the recommended search

parameters [8–12] have been used for solving various prob-

lems such as design of inhibitors [5], comparison of microtu-

bule-stabilizing agents [7] and exploring substrate binding

modes [8]. Because of the apparent success of the approach

[4–12], we decided to perform further systematic tests on a

set of 43 ligand–protein complexes which was previously used

in a comprehensive study on the selectivity of binding of aro-

matic compounds [13]**The AutoDock [2]-based blind docking (BD) approach [3] was introduced previously to search the entire surface of proteins for binding sites while simultaneously optimizing the conformations of the peptides. Each protein divide to three part and the search box for each part dedicated to be as big as possible, let the software make a biggest possible grid to search for potential binding pocket.**

The AutoDock [2]-based

blind docking (BD) approach [3] was introduced previously

to search the entire surface of proteins for binding sites while

simultaneously optimizing the conformations of the peptides.

The results of BD were regarded as “very encouraging” in a

recent review [4].BD[5–7] and the recommended search

parameters [8–12] have been used for solving various prob-

lems such as design of inhibitors [5], comparison of microtu-

bule-stabilizing agents [7] and exploring substrate binding

modes [8]. Because of the apparent success of the approach

[4–12], we decided to perform further systematic tests on a

set of 43 ligand–protein complexes which was previously used

in a comprehensive study on the selectivity of binding of aro-

matic compounds [13

### 3D structure preparation of complexes for MD simulation

**Scoulerine in the colchicine binding.** The complex designed in the first part of the present study consists of scoulerine bound in the colchicine-binding pocket of human α and βI tubulin heterodimers. A homology model allows to overcome the obstacle of not having a valid crystal structure for human α

(TBA1A_HUMAN) and βI tubulin (TBB5_HUMAN). Software package MOE2018 (Molecular Operating Environment, Inc) [35] was used to construct the procedure. The 1SA0 PDB crystal structure [36] was used as a structural template to create human α and βI tubulin heterodimers based on the corresponding sequence (UniProt: P07437) for human βI and (UniProt: Q71U36) for human α tubulin. The scoulerine structure was optimized by quantum mechanics molecular mechanics (QMMM) calculations. The pose of the drug was taken from the docked scoulerine to the colchicine binding site of the 1SA0 PDB crystal structure.

**Scoulerine in the laulimalide binding sites of microtubule.** The model used in the second part of the present study consists of scoulerine bound between two adjacent heterodimers. The homology models of human βI tubulin (TBB5_HUMAN) sequence (UniProt: P07437) and human α tubulin (TBA1A_HUMAN) sequence (UniProt: Q71U36) were generated by taking tubulin structures in 4O4H as a template [25]. The protofilament arrangement was based on the 2XRP crystal structure, which combined 8 Å resolution cryo-electron microscopy data with the 4O4H crystal structure, which has a resolution of 2.1 Å to obtain a microtubule structure at atomic resolution [25,37]. The scoulerine pose was taken from the docked scoulerine to laulimalide binding site on 4O4H.

**Molecular dynamic simulation.** In both complexes, parameters for the scoulerine were compatible with the general Amber force field (GAFF) and calculated *via* the antechamber suite of Amber 18 [38]. The Amber ff12SB force field was used to describe tubulin components. Each complex was solvated in an octahedral box of TIP3P water molecules [39] extending 12 Å from the solute. To obtain a 0.15 M ion concentration, sodium and chloride ions were added to neutralize the systems. The systems were gradually heated up to 310 K over 200 ps and maintained at 310 K for another 100 ps under constant volume conditions (NVT). The Langevin thermostat was used with a time collision frequency of 2 ps. Non-bonded terms were calculated within a 10 Å cut-off, except for long-range electrostatics, which was calculated with the particle mesh Ewald method [40]. During simulations, the SHAKE algorithm was used [41].

**Clustering analysis.** RMSD-based clustering was used to extract protein and ligand structures to represent the overall closeness and stability of a new inhibitor in the binding site. The movement trajectory of the complex was breakdown into clusters of similar sampled conformations during the MD simulation. The mass-weighted RMSD of the tubulin components, fit of the heavy atoms of the backbone of the protein, was calculated with respect to the structure at 0 ns. The clustering analysis was performed on each system, which was structurally equilibrated after 43 ns using one of the bottom-up algorithms, the average-linkage, in AmberTools18 (Figure 6 and 12) [42]. Several studies have discussed and validated the use of hierarchical algorithms in MD simulations [23,24]. A representative structure, centroid structures, was extracted for each cluster and used for comparative analyses [43].

**Microscale thermophoresis.** Microscale thermophoresis analyses were carried out using a Monolith NT.115 instrument (Nano Temper Technologies, Germany). Lyophilized tubulin powder was purchased

from commercial sources (Cytoskeleton Inc, Denver, CO, USA; T240) and reconstituted as previously described (Kalra et al., 2020). Briefly, 180 µL of GTP (guanosine triphosphate) supplemented BRB80 (80 mM PIPES pH 6.9, 2 mM $MgCl_2$, 0.5 mM EGTA, 1mM GTP) was first added to 20 µL of microtubule cushion buffer (BRB80T in 60 % glycerol). This solution was added to 1 g of lyophilized tubulin powder for reconstitution, aliquoted and stored at – 80$^o$ C. Rhodamine labelled tubulin (Cytoskeleton Inc, Denver, CO, USA; TL590m; 20 µg) was reconstituted by adding 70 µL of unlabelled tubulin solution (described above) to 5 µL of microtubule cushion buffer. All experiments were carried out at 23 $^o$C in Monolith NT.115 Premium capillaries (Nano Temper Technologies, cat# MO-L011), with 95% LED power (fluorescence lamp intensity) and 60% microscale thermophoresis power (IR-laser intensity). Scoulerine was diluted into the assay buffer containing 80 mM PIPES-KOH, pH 6.9, 2 mM $MgCl_2$ and 0.5 mM EGTA, with titration range of 50 µM to 12.2 nM. Experiments were performed in two replicates, data were analyzed by Monolith Affinity Analysis v2.2.6 software, exported to excel and plotted with GraphPad Prism 7.0.

# Result And Discussion

**Protonated or deprotonated scoulerine in cancer cell.** The first step to investigate the mechanism of action of scoulerine is to distinguish the proper structure for the ligand in the cancer cell environment. Scoulerine has a nitrogen atom in its ring that can be protonated in a sufficiently acidic environment. The acidity of cancer cells is slightly different from normal cells. *In vivo*, the extracellular matrix of tumours shows acidity of 6.2 to 6.9 pH. However, the intracellular matrix of tumours is alkaline, having a pH range of 7.12 to 7.65 [15]. With the help of quantum mechanical calculations, the total energies of scoulerine and protonated nitrogen scoulerine in acidic ($H_3O^+$) and basic ($OH^-$) environment, in vacuum and in the presence of water, were calculated and compared (Table 1). The total energies of -1161.73 a.u. for scoulerine and $H_2O$ versus -1161.63 a.u. for deprotonated scoulerine with hydroxy indicate that nitrogen of scoulerine stays deprotonated in the alkaline cancer cell environment.

Table 1. Total energy of protonated and non-protonated scoulerine by quantum mechanical calculations in 8 different systems. A) scoulerine and hydronium in vacuum and water. B) protonated scoulerine with $H_2O$ in water and vacuum C) scoulerine with $H_2O$ in water and vacuum D) protonated scoulerine with hydroxy in water and vacuum.

| A | $E_{Scoul}$ (a.u.) | $E_{H3O+}$ (a.u.) | $E_{Total}$(a.u.) | B | $E_{H^+\_Scoul}$ (a.u.) | $E_{H2O}$ (a.u.) | $E_{Total}$ (a.u.) |
|---|---|---|---|---|---|---|---|
| Vacuum | -1085.68 | -76.54 | -1162.22 | Vacuum | -1086.09 | -76.03 | -1162.11 |
| Water | -1085.70 | -76.54 | -1162.24 | Water | -1086.159 | -76.03 | -1162.19 |
| C | $E_{Scoul}$ (a.u.) | $E_{H2O}$ (a.u.) | $E_{Total}$ (a.u.) | D | $E_{H^+\_scoul}$ (a.u.) | $E_{HO^-}$ (a.u.) | $E_{Total}$ (a.u.) |
| Vacuum | -1085.68 | -76.03 | -1161.71 | Vacuum | -1086.09 | -75.33 | -1161.42 |
| Water | -1085.70 | -76.04 | -1161.73 | Water | -1086.16 | -75.48 | -1161.63 |

**Analysis of potential scoulerine binding sites on β tubulin.** The AutoDock software package was used [16] to test whether it is possible to find the potential binding sites and binding modes of flexible scoulerine on α and β tubulin monomers without any prior knowledge of their location and conformation. The AutoDock based blind docking (BD) approach [16] searches the entire surface of proteins for finding binding sites while simultaneously optimizing the conformations and the pose of the docked ligands. AutoDock is an appropriate tool for such a test because of its parameter set, based on the AMBER force field [17], and the capability of using flexible torsions for the ligands during the docking process. The protocol for docking procedures in different software packages is slightly different. In Autodock4, first the auto-grid program maps the target protein and then the auto-dock program docks the desired ligands to the set of grids of the mentioned protein [16].

Three potential binding sites were predicted as a result of blind docking of deprotonated scoulerine to 1SA0 PDB structure from Protein Data Bank (Figure 2). All of the three estimated binding sites found were on β tubulin. To investigate whether any of the predicted binding sites matched with the known binding sites of β tubulin, 41 Protein Data Bank files were superimposed on the 1SA0 PDB structure with scoulerine docked to the three predicted binding sites. Vinca alkaloids, colchicine, taxol, epothilone, and laulimalide sites are the major binding sites for most stabilizing and destabilizing tubulin inhibitors bind to prevent the dynamics of microtubules [18].

CN2, a colchicine derivative, from 1SA0 and colchicine from 5NM5, were found to be close to the docked scoulerine location in $S_1$. This observation suggests $S_1$ site has the potential to be a colchicine binding site. Laulimalide from 4O4H was also found to be close to the docked scoulerine location in $S_2$. Based on the analysis, the $S_2$ site can also potentially be a laulimalide binding pocket. For $S_3$, However, none of the available inhibitors were close enough to the docked scoulerine.

**Binding affinities and pose analysis of potential scoulerine binding sites.** To obtain numerical representatives for illustration of how close the potential binding sites are to the available colchicine and laulimalide binding sites, the RMSD values of scoulerine in $S_1$ and $S_2$ were calculated with respect to the

reference crystal structures of colchicine, CN2 (the colchicine derivative) and laulimalide form 5NM5,1SA0 and 4O4H PDB files, respectively.

In Table 3, the RMSD values of 3.5 and 3.4 Å between blind-docked scoulerine in S1 and crystal structure of colchicine (5MN5) and CN2 (1SA0) support the assumption and illustrate that the colchicine might share its binding site with scoulerine. Moreover, the RMSD values of 1.6 Å display even more adjacency between docked scoulerine in $S_2$ and the crystal structure of laulimalide (4O4H). To put to a test the strength of interactions between scoulerine and residues of the above-mentioned binding sites, colchicine and scoulerine were docked specifically to the colchicine binding site (1SA0) by Autodock and their binding affinities were then compared (Table 2). The same method was applied to calculate and compare the binding affinities of laulimalide and scoulerine to the only crystal structure that is available for laulimalide binding site (4O4H). The fact that a laulimalide docked between microtubule protofilaments and perhaps has two binding sites on β tubulin should not be overlooked (Table 2).

Binding affinity of -9.23 kcal/mol for colchicine versus -7.96 kcal/mol for scoulerine in the same binding site of b tubulin predicts weaker interactions between scoulerine and colchicine binding site of b tubulin. Scoulerine is a new chemotherapeutic drug and most of the biological aspect of the drug still needs to be evaluated. In 2018, the Habartova group used 20 mM of scoulerine to disrupt microtubule function in the A549 lung cancer cell line where nocodazole, another colchicine binding site inhibitor (CBSI), was used as control [6]. Nocodazole, at a concentration of 5 μM was shown to be as effective as scoulerine [5,19] Binding affinity of -7.5 kcal/mol for laulimalide versus -6.87 kcal/mol for scoulerine in the same binding site of β tubulin also predicted weaker binding interactions between scoulerine and b tubulin in the laulimalide binding sites of the 4O4H PDB crystal structure.

Table 2. A) Blinding energies of scoulerine and colchicine docked in the colchicine binding site (1SA0). B scoulerine and laulimalide docked in the laulimalide binding site (4O4H).

| | **Colchicine binding site A** | | **Laulimalide binding site B** | |
|---|---|---|---|---|
| Name | Colchicine | scoulerine | Laulimalide | scoulerine |
| B.A (kcal/mol) | -9.23 | - 7.96 | -7.50 | - 6.87 |

The steps described below were followed to evaluate the three potential binding sites of β tubulin and identify which one might be the most probable binding site for scoulerine. First, visualization of the docked poses of scoulerine was done. Next, analysis of the interacting residues of each binding site of β tubulin with scoulerine was carried out. Finally, results of molecular dynamics simulation of scoulerine in colchicine and laulimalide binding pockets were inspected.

Table 3. RMSD values for scoulerine in S1 and S2 with respect to the reference of crystal structures of colchicine, colchicine derivative, CN2 and laulimalide form 5NM5,1SA0 and 4O4H PDB files respectively.

| Crystal structure (Reference) | Docked scoulerine | RMSD (Å) |
|---|---|---|
| CN2 (1SA0) | $S_1$ | 3.4 |
| 5NM5 (Colchicine) | $S_1$ | 3.5 |
| Laulimalide (4O4H) | $S_2$ | 1.6 |

**Colchicine site.** The colchicine binding site on tubulin is a well-studied binding pocket and to date, many crystal structures of inhibitors have been found to dock in the colchicine binding site [20,21]. Seven pharmacophoric points were distinguished for CBSIs and are displayed in Figure 3. Based on previous work done on the subject, none of the known structures of CBSIs contains all seven pharmacophore groups [20,21]. Three hydrogen bond acceptors of pharmacophoric points are labelled as A1, A2 and A3 in Figure 3. The backbone nitrogen of Valα179 of colchicine binding pocket is in contact with A1. The sulfur atom of Cysβ239 interacts with A2. Finally, A3 forms one contact mainly with the backbone nitrogen of Alaβ248, Aspβ249, and Leuβ250. Hydrogen bond donor of pharmacophoric points, D1, interacts with the backbone oxygen of Thrα177. H1 and H2 are the two hydrophobic centers of pharmacophoric points. H1 point reacts to the side chains of Valα179 and Metβ257. H2 interacts with side chains of Leuβ255, Alaβ316, Valβ318 and Ileβ378. The last pharmacophoric points, R1, belong to one planar group (Figure 3) [20,21].

**Potential scoulerine binding site ($S_1$).** In Figure 4.A, a two-dimensional interaction scheme of the superimposed colchicine crystal structure from 5NM5 PDB file (green) on scoulerine in the $S_1$ site (red) illustrates the pose of scoulerine in comparison to the pose of colchicine. Even though the pose of the colchicine crystal structure overlaps with the pose of scoulerine in the $S_1$ (Figure 4.A), analyzing the adaptation of scoulerine with seven pharmacophore groups of colchicine binding site inhibitors was essential. The two-dimensional interaction scheme (Figure 4.B) displays interactions between scoulerine and potentially a binding pocket, $S_1$. Scoulerine has the A1 pharmacophoric point of CBSI ligands because of the hydrogen acceptor interaction between a sulfur atom of Cys239 with N of scoulerine. The A3 pharmacophoric point of CBSI ligands is supposed to have a hydrogen acceptor by the backbone nitrogen of Ala248 or Leu250. However, the distance between the backbone nitrogen of Ala248 or Leu250 and scoulerine is 4.2 Å that translates into weak electrostatic interactions. Taking into consideration that the pose of scoulerine is the result of wide blind docking, there is a possibility that a small adjustment might lead to the hydrogen bonding with either Ala248 or Leu250 (Figure 4.B). The third pharmacophoric point of CBSI, H2, is a hydrophobic center that interacts with side chains of Leu255, Ala316, Val318, and Ile378. The green color of the above-mentioned residues in the 2-dimensional interaction scheme in Figure 4.B means greasy that refer to hydrophobic nature of the residues. The blue circles show the ligand exposure to the solvent and the dotted line around the ligand shows the proximity contour. The closer is the ligand to the contour in the scheme, the deeper the ligand is in the cavity of the binding

pocket of the protein. To put it in a better perspective, Figure 4.C is generated to show the hydrophobic surface of protein in the $S_1$ site that wraps the hydrophobic center, H2, of the scoulerine.

Scoulerine also has planar group to fit the pharmacophoric R1 point. D1 and A1 of the pharmacophoric points of CBSI interact with Thr177 and Val178 of α tubulin. However, the closest residue of α tubulin in the Figure 4.B is Ser178.

## Conformational analysis

**RMSD analysis on $S_1$ site.** Homology model of human α and βI tubulin based on 1SA0 template was performed. Scoulerine was specifically docked to colchicine binding site. Molecular dynamic simulation of the system was performed for 120 ns. The RMSD values of scoulerine to the backbone of colchicine binding site were calculated during the simulation. In order to assess the equilibration of the system, the plot of total energies of the system versus time was plotted and compared to the RMSD plot. The system appeared to be equilibrated after 43 ns. The RMSD value of 2.2 to 2.3 Å for 77 ns of simulation after the equilibration verified that the interactions between scoulerine and residues of colchicine binding site are strong enough to keep the ligand close to binding pocket (Figure 5).

**Clustering analysis.** Clustering analysis was carried out with the hierarchical agglomerative algorithm [22]. Several studies have discussed and validated the use of hierarchical algorithms in MD simulations [23,24]. The frames of 77 ns were clustered as reported by binding site closeness. To be specific, this closeness was sorted based on the mass-weighted RMSD of the binding-site atoms, which includes scoulerine and residues having atoms within 8 Å of scoulerine. The centroid structures have the smallest RMSD relative to all the other members of the same cluster.

The algorithm generates representative structures, centroid structures, of scoulerine poses in the colchicine binding site throughout the 77 ns simulation. The trajectory frames were partitioned into clusters A, B, and C (Figure 6). Cluster B of the graph indicates more than 50 percent of occupancy during the simulation. In Figure 7.A, the post of the representative structure of dominant cluster B was displayed with the pose of colchicine's crystal structure (Figure 7.D) of 5NM5 structure. The representative structure (centroid) for each cluster was extracted and displayed in (Figure 7.C).

As displayed in Figure 7.B, the sulfur atom of Cysβ239 still has a hydrogen acceptor with scoulerine (A2). As predicted before, the backbone nitrogen of Leuβ250 now is sufficiently close to make a hydrogen binding with scoulerine (A3). Hydrophobic interactions between scoulerine (H2) with side chains of Leu255, Val318, and Ile378 still occurred as illustrated in Figure 7.E. The hydrogen bond donor D1 pharmacophoric point of colchicine binding site inhibitors did not appear in the interaction diagram of blindly docked scoulerine to α and β tubulin. D1 interacts with the backbone oxygen of Thrα177. However,

the interaction diagram of the most dominant representative structure of scoulerine docked to colchicine binding site of human α and βI tubulin over 77 ns of MD simulation shows Thrα177 near enough to the ligand to demonstrate weak electrostatic interaction.

**Laulimalide sites on β tubulin.** Laulimalide is a novel microtubule stabilizer that binds between two protofilaments of a microtubule, which has been in the spotlight because of its unique mode of action. Despite computational studies which attempted to identify the laulimalide binding site, the first crystal structure of laulimalide bound to tubulin was captured by x-ray diffraction in 2014. The binding pocket formed by residues Gln293, Phe296, Pro307, Arg308, Tyr312, Val335, Asn339, Tyr342, Ser298, Asp297, and Phe343 of tubulin (Figure 8). Gln293, Ser298, Asp297, and Asn339 are the residues that make hydrogen binding with laulimalide [22,25,26].

Computational studies on the mode of action of laulimalide discovered Gln293, Phe296, and Asn 339 residues of β tubulin as the most stabilizing residues [22,25,26].

The computational analyses also showed that Lys122, Glu125, Ser126, and Arg121 residues of β tubulin of adjacent protofilament bind to laulimalide but they have smaller stabilizing contribution [22,25,26].

Similar to colchicine binding pocket, laulimalide is not the only inhibitor that binds to laulimalide binding sites. Peloruside (4O4L PDB) is another drug that binds to the laulimalide binding site of β tubulin and identified by x-ray diffraction. The binding mode of peloruside and laulimalide to tubulin is homogeneous. In this case, Ser298, Asp297, Arg308, Gln293, and Tyr312 residues of tubulin formed hydrogen bonds with peloruside. Gln293, Ser298, and Asp297 residues are special since they make hydrogen bonding with both of inhibitors, laulimalide and peloruside [25].

**Potential scoulerine binding site ($S_2$).** Based on blind docking results, the O37 of the hydroxyl group of scoulerine in the binding site $S_2$, similar to laulimalide and peloruside, makes hydrogen-donor bonds with the side chains of Gln293 (Figure 9.A). Asp297 of laulimalide binding pocket also forms hydrogen bonds with laulimalide and peloruside. However, in the interaction of scoulerine with the residues of $S_2$ site, Asp297 shows electrostatic interaction instead. Pro307, Arg308, Val335, Lys338, Phe296, and Asn339 are other interactive residues of $S_2$ site that held in common with the residues of laulimalide binding site. In Figure 9.B, a two-dimensional interaction scheme of superimposed laulimalide crystal structure from 4O4H PDB file (green) on scoulerine in the $S_2$ site (red) illustrates the pose of scoulerine in a comparison with the pose of laulimalide.

The computational analyses also showed that Lys122, Glu125, Ser126, and Arg121 residues of β tubulin of adjacent protofilament bind to laulimalide but they have smaller stabilizing contribution.

The $S_3$ site primarily appears by blind docking of scoulerine to 1SA0 PDB structure and did not show any compatibility with available binding sites of β tubulin by crystallography (Figure 9.C). The residues of the

$S_3$ site, Arg123, Lys124, Glu127, and Ser128, are very similar to the residues of the second binding site of laulimalide on β tubulin of adjacent protofilament, namely Lys122, Glu125, Ser126, and Arg121.

## Conformational analysis

**RMSD analysis on scoulerine bound between protofilament (laulimalide binding sites**). Homology model of human α and βI tubulins based on 4O4H crystal structure combined with the 2XRP crystal structure to arrange two adjacent protofilament. The scoulerine pose was taken from the docked scoulerine to Laulimalide binding site on 4O4H [25].

Molecular dynamics simulation of the system was performed for 160 ns. The RMSD values of scoulerine to the backbone of the laulimalide binding site were calculated during the simulation (Figure 10). In order to assess the system's equilibration, the plot of total energies of the system versus time was graphed and compared to the RMSD plot. The system appeared to be equilibrated after 10 ns but since substantial structural equilibration (45 ns) is necessary to stabilize the lateral contacts between tubulin heterodimers, production data were collected for 115 ns after equilibration. The RMSD value of 3.1 to 3.3 Å for 115 ns of simulation verified that the interactions between scoulerine and residues of scoulerine binding site are strong enough to keep the ligand close to the binding pocket.

**Clustering Analysis.** Same as for the colchicine binding site, clustering analysis was also conducted for the frames of the last 115 ns of the simulation to show the stability of the system to keep the ligand in the binding pockets. The mass-weighted RMSD of the binding-site atoms throughout the trajectory frames of 115 ns were classified after equilibration to two clusters. To be specific, the binding-site atoms include scoulerine and residues having atoms within 8 Å of scoulerine, water and ions are excluded. The algorithm also generates two representative structures of scoulerine poses in the laulimalide binding sites between the protofilament for each of the clusters (Figure 11). Cluster A of the graph indicates more than 67 percent of occupancy during the simulation.

Representative structures of scoulerine between $\alpha_A$ $\beta_A$ and $\alpha_B$ $\beta_B$ tubulins of two adjacent protofilaments are displayed in Figure 12.C. Representative structures for cluster A are shown in purple and in dark pink colour for cluster B.

In Figure 12.A, the representative structure of dominant cluster A was displayed with superimposed laulimalide crystal structure of the 4O4H structure. The residues of laulimalide's binding pocket of $\beta_B$ tubulin are highlighted in light green. The computational study illustrated the residues of the second binding site of laulimalide on the adjacent $\beta_A$ tubulin and they are coloured dark green in Figure 12.A [22].

The 2D interaction scheme of the most dominant representative structure of the system shows that scoulerine can also bind between β tubulins of two adjacent protofilaments (Figure 12.B). The hydrogen acceptor between the nitrogen of the scoulerine and Gln293 of β tubulin and π-hydrogen interaction between a ring of scoulerine and Ser125 of $\beta_A$ tubulin, are the two most important binding interactions between scoulerine and residues of laulimalide binding pockets. Gln293, Phe296, and Asn339 residues of β tubulin are the most important stabilizer residues in the binding interaction between laulimalides and residues of its binding sites. The involvement of all three residues in the interaction scheme of scoulerine with laulimalide binding sites [22,26] raised the possibility that scoulerine might be a new inhibitor to bind between microtubules. Val335 and Phe296 residues of laulimalide binding site also showed weak electrostatic interaction with scoulerine. As shown in Figure 12.A, scoulerine has smaller-scale structure compared to laulimalide. Thus, the new drug shifted from the first binding pocket of laulimalide on $\beta_B$ tubulin, the crystal structure of laulimalide binding site 4O4H PDB, toward the second one on $\beta_A$ tubulin to be able to bind to both binding sites. Lys122, Glu125, and Ser126 are the most important residues on laulimalide binding pocket on $\beta_A$ tubulin [22,26] which also interact with scoulerine (Figure 12.A and B).

**Experimental validation.** Based on the computational prediction, scoulerine potentially should be able to bind to both colchicine and laulimalide binding sites. However, based on docking results, the binding affinities might not be as strong as the colchicine or laulimalide.

To evaluate the educated estimation, the dissociation constant of scoulerine bound to free α and b tubulin dimers and microtubules were calculated by the microscale thermophoresis method. The $K_d$ values of $35.9 \times 10^{-6}$ M and $431 \times 10^{-6}$M were reported for scoulerine bound to labelled free a and b tubulin dimers and labelled microtubules, respectively (Figure 13.A)

The range of values for the reported dissociation constants confirms the computational results and indicates that scoulerine can bind to both free tubulin dimers and microtubules. Consequently, it has a dual mechanism of action.

The dissociation constant, $K_d$, of the well-studied colchicine bound to free a and β tubulin dimers were also measured to use as a reference. The $K_d$ value of $67.6 \times 10^{-6}$ M shows that colchicine's binding affinity is stronger than that of the scoulerine in the interaction with tubulin dimers (Figure 13.B). The binding affinities calculated *via* docking were reported to be -9.32, -7.96, and -6.87 kcal/mol for colchicine and scoulerine in colchicine and laulimalide binding sites, respectively (Table 2). Unfortunately, due to extreme difficulty in obtaining samples of laulimalide, we have not been able to test its binding affinity for tubulin in microtubules in this assay but it has been reported elsewhere [27]. The range of values of binding affinities agrees with dissociation constant values.

# Conclusion

Scoulerine is a natural drug in the family of isoquinoline alkaloids that can be extracted from Croton flavens [28], Corydalis dubia [29], and Corydalis cava [10,30]. New research on scoulerine has revealed a range of effects, including anti-proliferative and pro-apoptotic properties, as well as antimitotic activity that disrupts microtubules [5,6]. The listed properties of scoulerine make it a possible candidate for use in cancer treatment. However, the mode of action of the scoulerine is still unclear to date. The present work attempted to predict the mechanism of action of this new chemotherapeutic agent by computational approach. A combination of blind docking and molecular dynamics provides a useful approach to acquire new, detailed information about the interactions between scoulerine and b tubulin within a microtubule. Three potentially binding sites were found on b tubulin of microtubule *via* blind docking method. With the help of RMSD between the crystallographic structure of inhibitors of b tubulin and the docked ligand conformations, three possible binding sites have been discovered and labelled $S_1$,$S_2$, and $S_3$ (Figure 2). The residues of the discovered $S_1$ binding site on b tubulin are mostly the same as the colchicine binding pocket.

Laulimalide is a unique stabilizer of the microtubule that can bind to b tubulins of adjacent protofilament [22]. The residues of estimated $S_2$ and $S_3$ of b tubulins have similarities with the laulimalide binding site on b tubulins of adjacent protofilament. Two improved models of scoulerine binding to ab tubulin heterodimers were designed and investigated by molecular dynamic simulations. The first one consists of scoulerine located between a and b tubulins in the crystallographic colchicine binding sites based on 1SA0 PDB. In the second one, scoulerine is placed between two adjacent ab heterodimers and bound to a crystallographic laulimalide binding site based on 4O4H PDB. The cluster analyses were calculated for both of the systems. The structures of the smallest RMSD of each of the clusters were also presented. The 3D interaction scheme of the representative structure of the highest cluster for both systems is also displayed. The results showed scoulerine can bind between both a and b tubulin of a heterodimer. It can also bind between b tubulins of two adjacent heterodimers. The mentioned prediction was put to test by measuring the dissociation constant between scoulerine bound to labelled free and tubulin dimers and labelled microtubules. The $K_d$ value of $35.9 \times 10^{-6}$ M and $431 \times 10^{-6}$M was reported for scoulerine bound to labelled free a and b tubulin dimers and labelled microtubules. The similarity between the values of the $K_d$ for both systems confirmed the computational estimations and illustrated that scoulerine might have a dual mechanism of action both as microtubule stabilizer in the laulimalide binding sites and an inhibitor of microtubule polymerization which binds in the colchicine binding site. This places scoulerine in a unique category of tubulin-binding agents.

# Declarations

### Data availability

All data that generated or analysed during this study are available from the corresponding authors upon justified request.

### Acknowledgements

J.A.T and M.K. gratefully acknowledge funding support for this project received from NSERC (Canada).

The use of resources provided by WestGrid (www.westgrid.ca)

and Compute Canada (www.computecanada.ca) is gratefully acknowledged

### Author contributions

J.A.T. conceived the project. M. Mo. did all calculations and data analysis. Q.W. and M. Mi. did the experimental validation. M. Mo., M.K. and J.A.T. outlined calculations. M. Mi. provided laboratory infrastructure and reagents for the experimental assays. M. Mo. wrote the first draft of manuscript, and M.K. and J.A.T. managed all aspects of the writing, including final draft preparation. All authors reviewed the manuscript.

### Competing interests

The authors declare no competing interests.

## References

1. Cragg, G. M. & Pezzuto, J. M. Natural Products as a Vital Source for the Discovery of Cancer Chemotherapeutic and Chemopreventive Agents. *Med. Princ. Pract.* **25**, 41–59 (2016).
2. Liu, D., Meng, X., Wu, D., Qiu, Z. & Luo, H. A Natural Isoquinoline Alkaloid With Antitumor Activity: Studies of the Biological Activities of Berberine. *Front. Pharmacol.* **10**, 9 (2019).
3. Tian, J. *et al.* Scoulerine promotes cell viability reduction and apoptosis by activating ROS-dependent endoplasmic reticulum stress in colorectal cancer cells. *Chem. Biol. Interact.* **327**, 109184 (2020).
4. Kukula-Koch, W. A., Widelski, J. & Alkaloids. in Pharmacognosy (eds. Badal, S. & Delgoda, R.)163–198(Elsevier, 2017).
5. Habartova, K. *et al.* Scoulerine affects microtubule structure, inhibits proliferation, arrests cell cycle and thus culminates in the apoptotic death of cancer cells. *Sci. Rep.* **8**, 4829 (2018).
6. Hagel, J. M. *et al.* Transcriptome analysis of 20 taxonomically related benzylisoquinoline alkaloid-producing plants. *BMC Plant Biol.* **15**, 227 (2015).
7. Alisaraie, L. & Tuszynski, J. A. Determination of noscapine's localization and interaction with the tubulin-α/β heterodimer. *Chem. Biol. Drug Des.* **78**, 535–546 (2011).
8. Ghaly, P. E., El-Magd, A., Churchill, R. M., Tuszynski, C. D. M., West, F. & J. A. & G. A new antiproliferative noscapine analogue: chemical synthesis and biological evaluation. *Oncotarget.* **7**, 40518–40530 (2016).
9. Ghaly, P. E. *et al.* Synthesis and biological evaluation of structurally simplified noscapine analogues as microtubule binding agents. *Can. J. Chem.* **95**, 649–655 (2017).

10. Chlebek, J. *et al.* Application of BACE1 immobilized enzyme reactor for the characterization of multifunctional alkaloids from Corydalis cava (Fumariaceae) as Alzheimer's disease targets. *Fitoterapia.* **109**, 241–247 (2016).
11. Kumar, B., Kumar, R., Skvortsova, I. & Kumar, V. Mechanisms of Tubulin Binding Ligands to Target Cancer Cells: Updates on their Therapeutic Potential and Clinical Trials. *Curr. Cancer Drug Targets.* **17**, 357–375 (2017).
12. Dustin, P. The Role of MT in Mitosis. in *Microtubules* 340–397 (Springer, 1978).
13. Rohena, C. C. & Mooberry, S. L. Recent progress with microtubule stabilizers: new compounds, binding modes and cellular activities. *Nat. Prod. Rep.* **31**, 335–355 (2014).
14. Prota, A. E. *et al.* A new tubulin-binding site and pharmacophore for microtubule-destabilizing anticancer drugs. Proc. Natl. Acad. Sci. U. S. A. 111, 13817–21(2014).
15. Koltai, T. Cancer: fundamentals behind pH targeting and the double-edged approach. *Onco. Targets. Ther.* **9**, 6343–6360 (2016).
16. Morris, G. M. *et al.* AutoDock4 and AutoDockTools4: Automated docking with selective receptor flexibility. *J. Comput. Chem.* **30**, 2785–2791 (2009).
17. Cornell, W. D. *et al.* A Second Generation Force Field for the Simulation of Proteins, Nucleic Acids, and Organic Molecules. *J. Am. Chem. Soc.* **117**, 5179–5197 (1995).
18. Morris, P. G. & Fornier, M. N. Microtubule active agents: beyond the taxane frontier. *Clin. Cancer Res.* **14**, 7167–7172 (2008).
19. Wang, Y. *et al.* Structures of a diverse set of colchicine binding site inhibitors in complex with tubulin provide a rationale for drug discovery. *FEBS J.* **283**, 102–111 (2016).
20. Lu, Y., Chen, J., Xiao, M., Li, W. & Miller, D. D. An overview of tubulin inhibitors that interact with the colchicine binding site. *Pharm. Res.* **29**, 2943–2971 (2012).
21. O'Boyle, N. M. *et al.* Synthesis and evaluation of azetidinone analogues of combretastatin A-4 as tubulin targeting agents. *J. Med. Chem.* **53**, 8569–8584 (2010).
22. Churchill, C. D. M., Klobukowski, M. & Tuszynski, J. A. The Unique Binding Mode of Laulimalide to Two Tubulin Protofilaments. *Chem. Biol. Drug Des.* **86**, 190–199 (2015).
23. Demir, Ã. *et al.* Ensemble-based computational approach discriminates functional activity of p53 cancer and rescue mutants. *PLoS Comput. Biol.* **7**, e1002238 (2011).
24. Shao, J., Tanner, S. W., Thompson, N. & Cheatham, T. E. Clustering Molecular Dynamics Trajectories: 1. Characterizing the Performance of Different Clustering Algorithms. *J. Chem. Theory Comput.* **3**, 2312–2334 (2007).
25. Prota, A. E. *et al.* Structural basis of microtubule stabilization by laulimalide and peloruside A. *Angew. Chem. Int. Ed. Engl.* **53**, 1621–1625 (2014).
26. Churchill, C. D. M., Klobukowski, M. & Tuszynski, J. A. Analysis of the binding mode of laulimalide to microtubules: Establishing a laulimalide-tubulin pharmacophore. *J. Biomol. Struct. Dyn.* **34**, 1455–1469 (2016).

27. Pryor, D. E. *et al.* The microtubule stabilizing agent laulimalide does not bind in the taxoid site, kills cells resistant to paclitaxel and epothilones, and may not require its epoxide moiety for activity. *Biochemistry.* **41**, 9109–9115 (2002).
28. Eisenreich, W. J., Höfner, G. & Bracher, F. Alkaloids from Croton flavens L. and their affinities to GABA-receptors. *Nat. Prod. Res.* **17**, 437–440 (2003).
29. Wangchuk, P., Keller, P. A., Pyne, S. G., Willis, A. C. & Kamchonwongpaisan, S. Antimalarial alkaloids from a Bhutanese traditional medicinal plant Corydalis dubia. *J. Ethnopharmacol.* **143**, 310–313 (2012).
30. Chlebek, J. *et al.* Acetylcholinesterase and Butyrylcholinesterase Inhibitory Compounds from Corydalis Cava (Fumariaceae). *Nat. Prod. Commun.* **6**, 607–610 (2011).
31. Dunning, T. H. Gaussian basis sets for use in correlated molecular calculations. I. The atoms boron through neon and hydrogen. *J. Chem. Phys.* **90**, 1007–1023 (1989).
32. Schmidt, M. W. *et al.* General atomic and molecular electronic structure system. *J. Comput. Chem.* **14**, 1347–1363 (1993).
33. Gordon, M. S. & Schmidt, M. W. Advances in electronic structure theory: GAMESS a decade later. in *Theory and Applications of Computational Chemistry* (eds. Dykstra, C. E., Frenking, G., Kim, K. S. & Scuseria, G. E.) 1167–1189 (Elsevier, 2005).
34. Barca, G. M. J. *et al.* Recent developments in the general atomic and molecular electronic structure system. *J. Chem. Phys.* **152**, 154102 (2020).
35. Autodock. (Chemical Computing Group ULC & Montreal Canada 2018).
36. Ravelli, R. B. G. *et al.* Insight into tubulin regulation from a complex with colchicine and a stathmin-like domain. *Nature.* **428**, 198–202 (2004).
37. Fourniol, F. J. *et al.* Template-free 13-protofilament microtubule-MAP assembly visualized at 8 A resolution. *J. Cell Biol.* **191**, 463–470 (2010).
38. Wang, J., Wolf, R. M., Caldwell, J. W., Kollman, P. A. & Case, D. A. Development and testing of a general amber force field. *J. Comput. Chem.* **25**, 1157–1174 (2004).
39. Jorgensen, W. L., Chandrasekhar, J., Madura, J. D., Impey, R. W. & Klein, M. L. Comparison of simple potential functions for simulating liquid water. *J. Chem. Phys.* **79**, 926–935 (1983).
40. Essmann, U. *et al.* A smooth particle mesh Ewald method. *J. Chem. Phys.* **103**, 8577–8593 (1995).
41. Ryckaert, J. P., Ciccotti, G. & Berendsen, H. J. Numerical integration of the cartesian equations of motion of a system with constraints: molecular dynamics of n-alkanes. *J. Comput. Phys.* **23**, 327–341 (1977).
42. Case, D. A. *et al.* R. &, D.M., P. A. K. AMBER 2018, University of California, San Francisco. (2018).
43. Lepre, M. G. *et al.* Insights into the Effect of the G245S Single Point Mutation on the Structure of p53 and the Binding of the Protein to DNA.*Molecules***22**, (2017).

# Figures

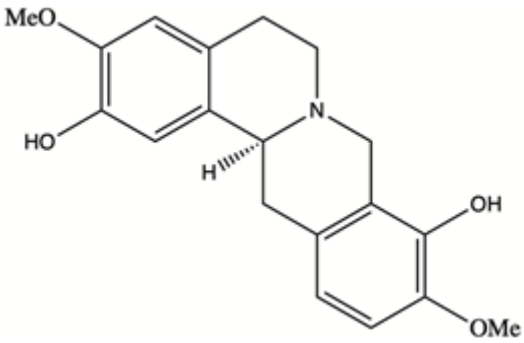


**Figure 1**

Scoulerine structure

**Figure 2**

S1, S2 and S3 represent the three predicted potential binding sites by blink docking of scoulerine (blue) to α (green) and β (red) tubulins of 1SA0 PDB structure. Colchicine derivative from 1SA0 in S1 and Laulimalide from 404H in S2 shown in white.

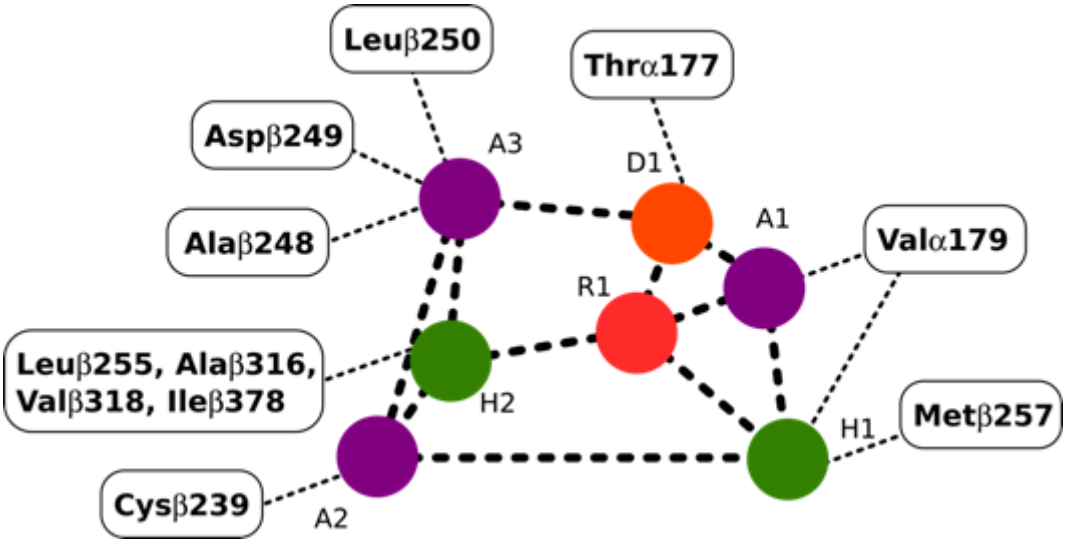

## Figure 3

Interactions between the pharmacophoric points and the tubulin structure 21.

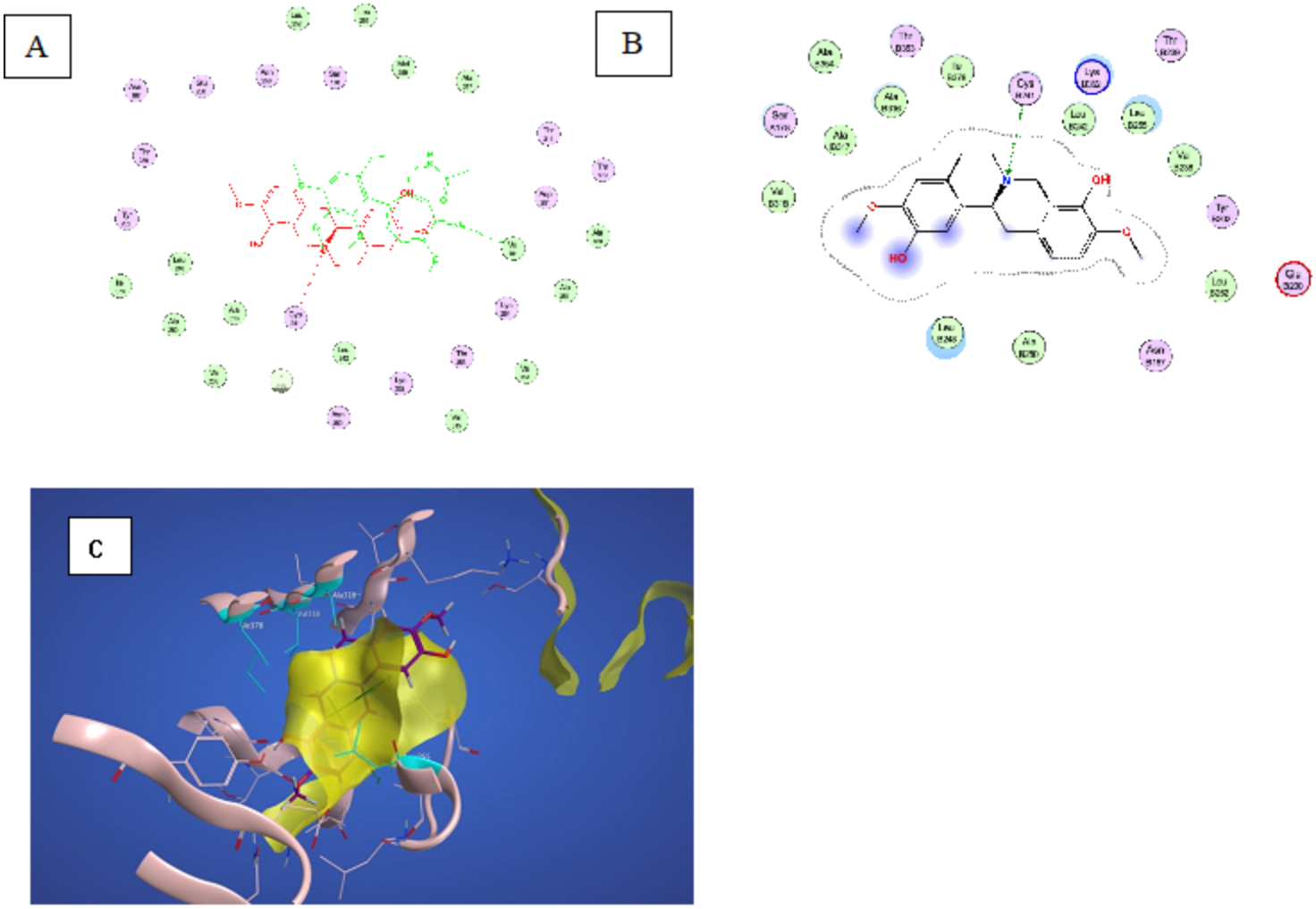


## Figure 4

A) 2D-interaction scheme of superimposed colchicine crystal structure from 5NM5 PDB file (green) on scoulerine in the S1 site (red). B) 2D-interaction scheme of scoulerine in the S1 site. C) Surface patches identifying regions of hydrophobicity (yellow) around scoulerine. Residues Leu255, Ala316, Val318, and Ile378 of β tubulin that involve in hydrophobic interaction colored in teal.

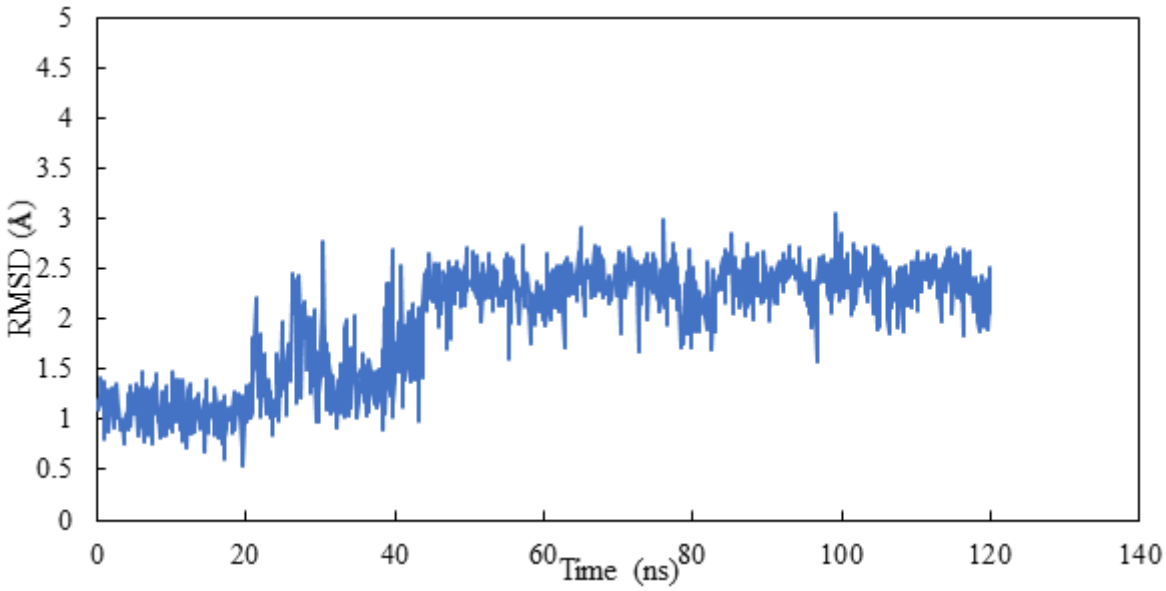


**Figure 5**

RMSD of scoulerine to the colchicine binding site (S1-1SA0).

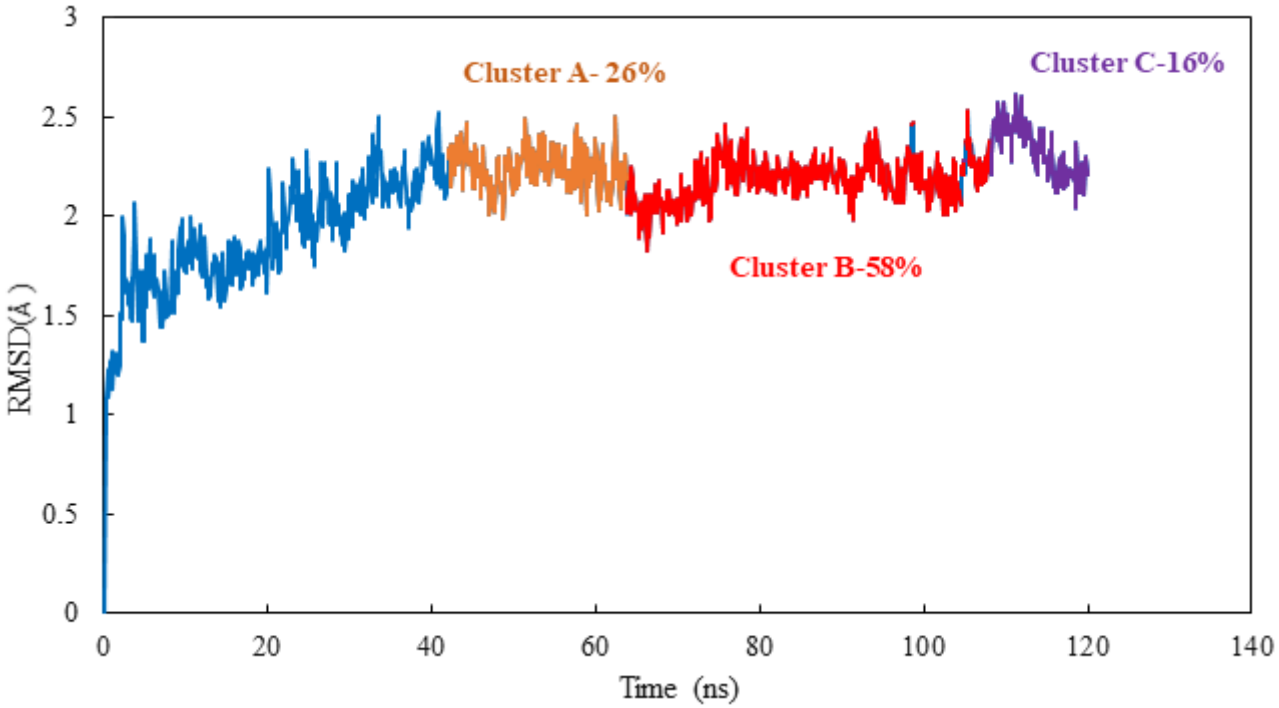


**Figure 6**

Mass-weighted root mean squared deviation (Å) of the binding site of colchicine to tubulin, classified according to cluster number, with occupancy indicated. The binding site includes scoulerine and residues having atoms within 8 Å of scoulerine. The dark blue part of the graph illustrates the equilibration.

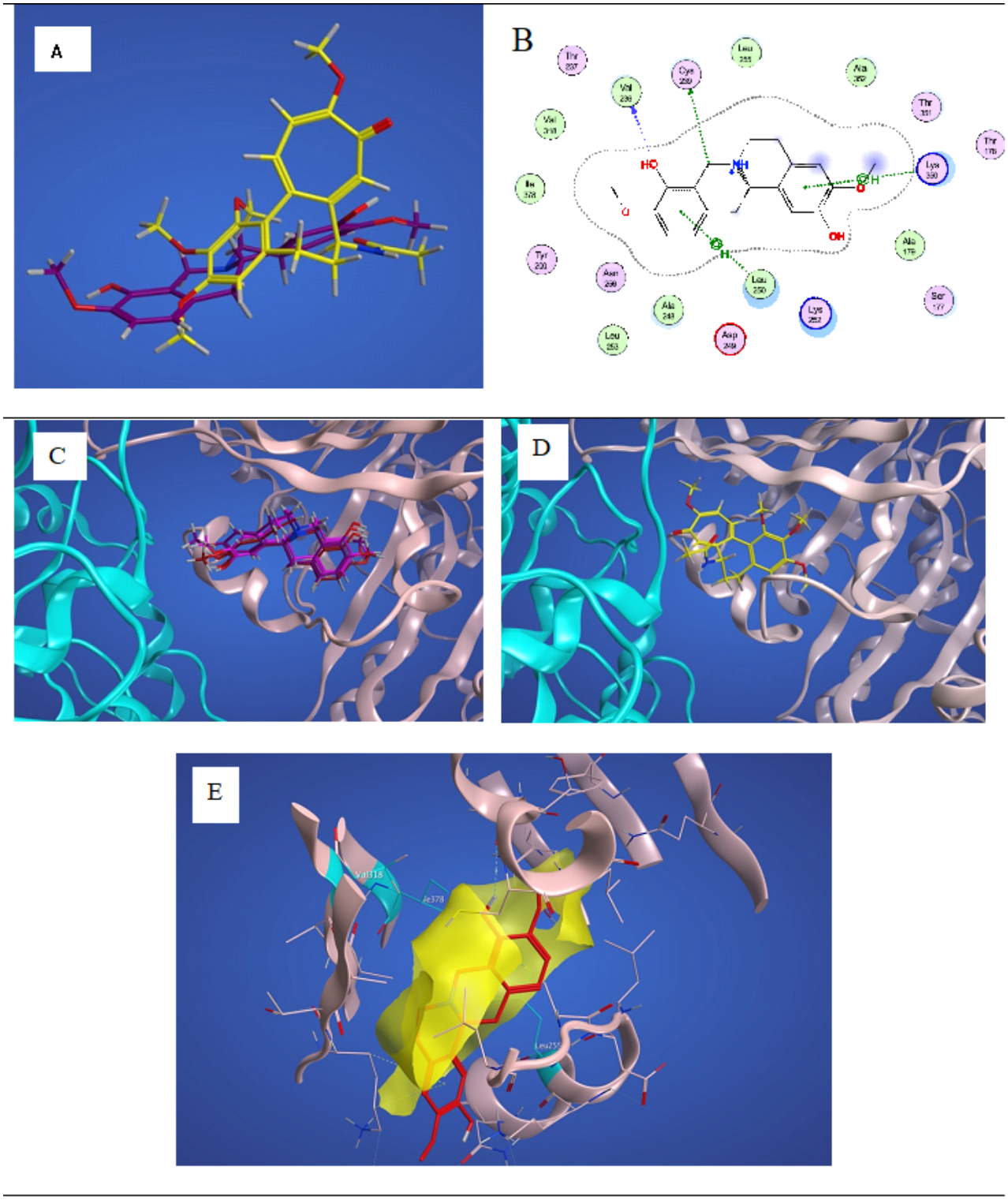


## Figure 7

A) Representative structures of scoulerine in cluster B (purple) versus colchicine (yellow) B) 2D-interaction scheme of scoulerine in colchicine binding site. C) Representative structures of cluster A (red), cluster B (purple) and cluster C (dark pink) in colchicine binding site, α tubulin colored in teal and βI tubulin colored in light pink. D) Colchicine (yellow) in colchicine binding site, α tubulin colored in teal and βI tubulin colored in light pink. E) surface patches identifying regions of hydrophobicity (yellow) around

scoulerine, residues Leu255, Val318, and Ile378 of β tubulin that involve in hydrophobic interaction colored in teal.

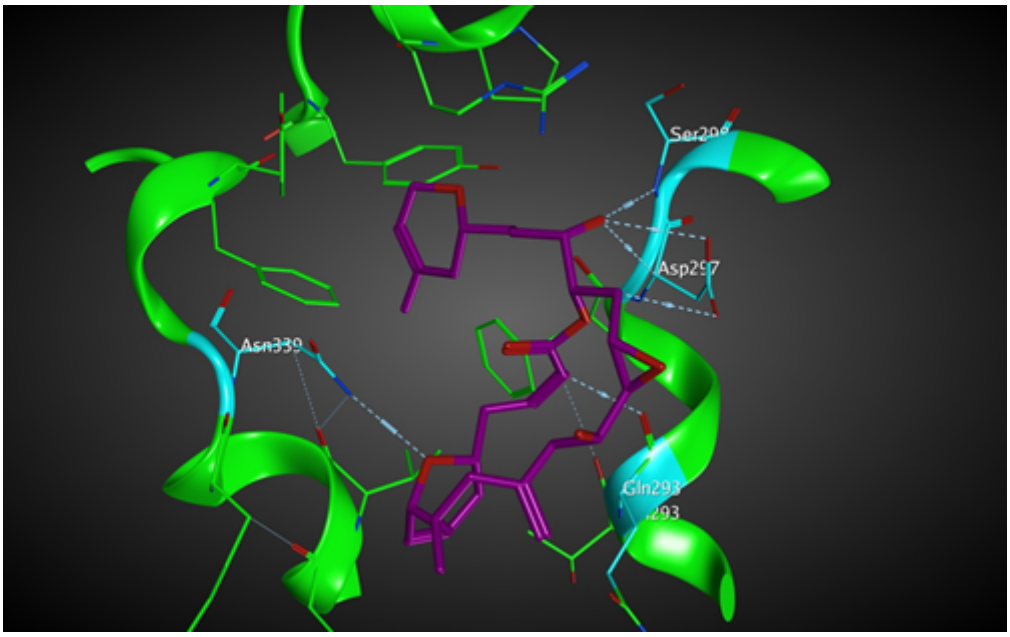


## Figure 8

Laulimalide in the laulimalide binding site of β tubulin (green) in 4O4H PDB file. Residues in blue have hydrogen bonding interaction with laulimalide (purple).

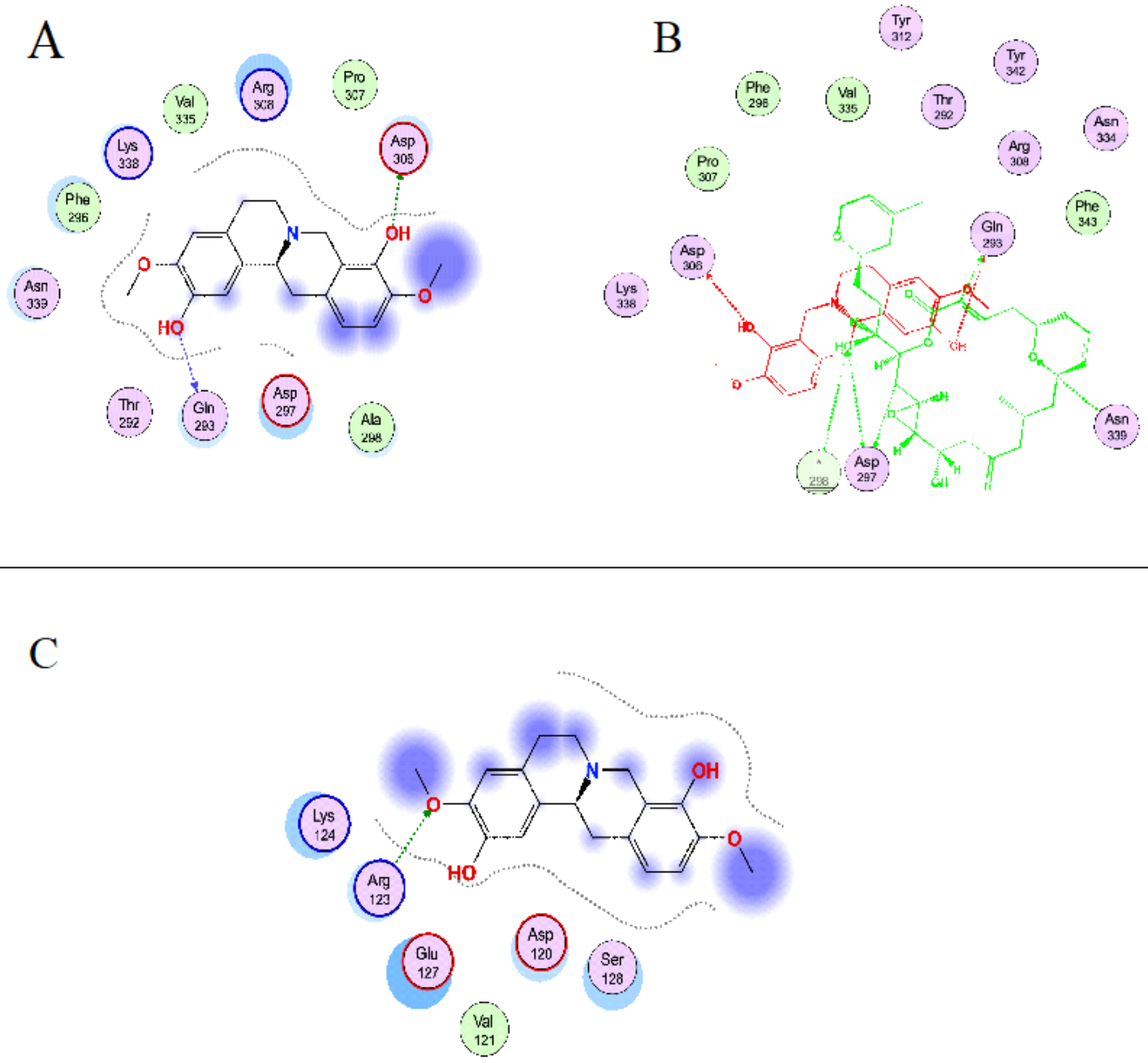


1

## Figure 9

A) 2D-interaction scheme of scoulerine in the S2 site via blind docking. B) 2D-interaction scheme of superimposed laulimalide crystal structure from 4O4H PDB file (green) on scoulerine (red) in the S2 site. C) 2D- interaction scheme of scoulerine in the S3 site via blind docking.

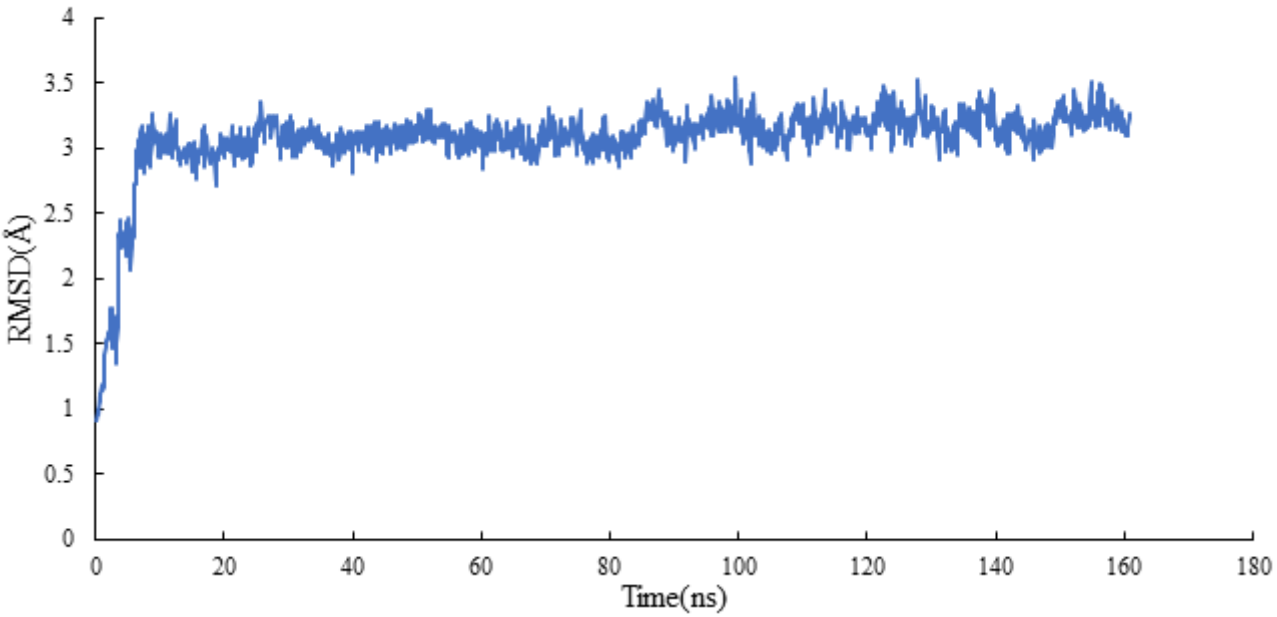


## Figure 10

RMSD of scoulerine to the Colchicine binding site (S1-1SA0).

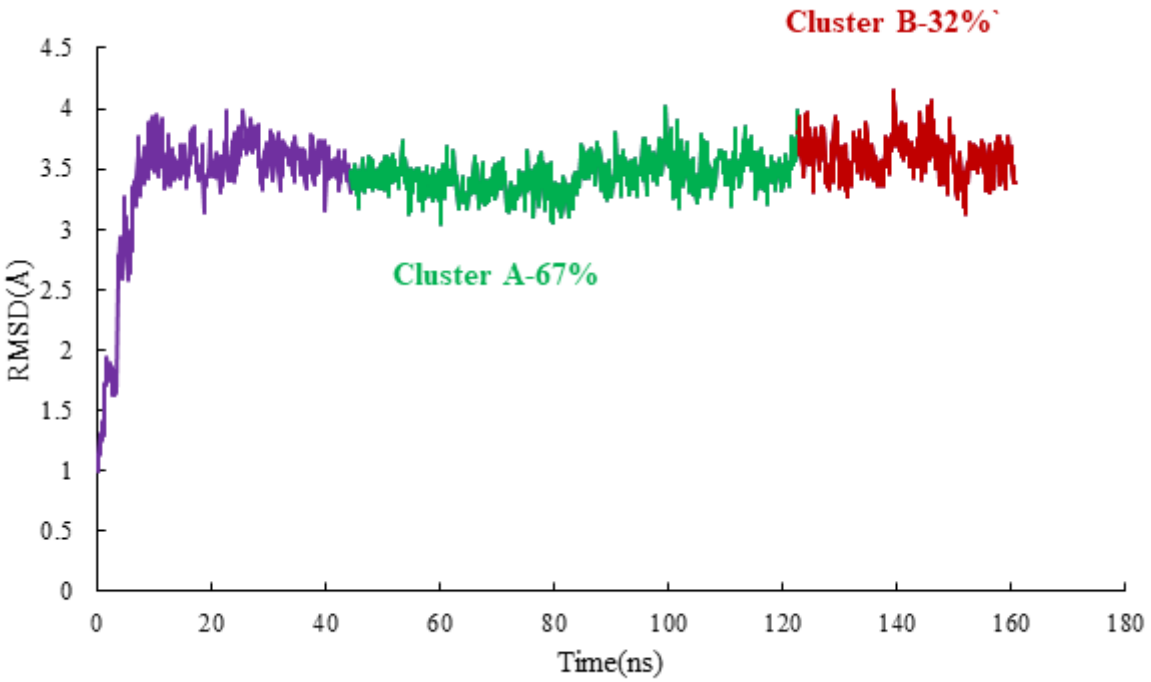


## Figure 11

Mass-weighted root mean squared deviation (Å) of the binding sites of laulimalide to tubulin, classified according to cluster number, with occupancy indicated. The binding site includes scoulerine and residues having atoms within 8 Å of scoulerine. The purple part of the graph illustrates the equilibration.

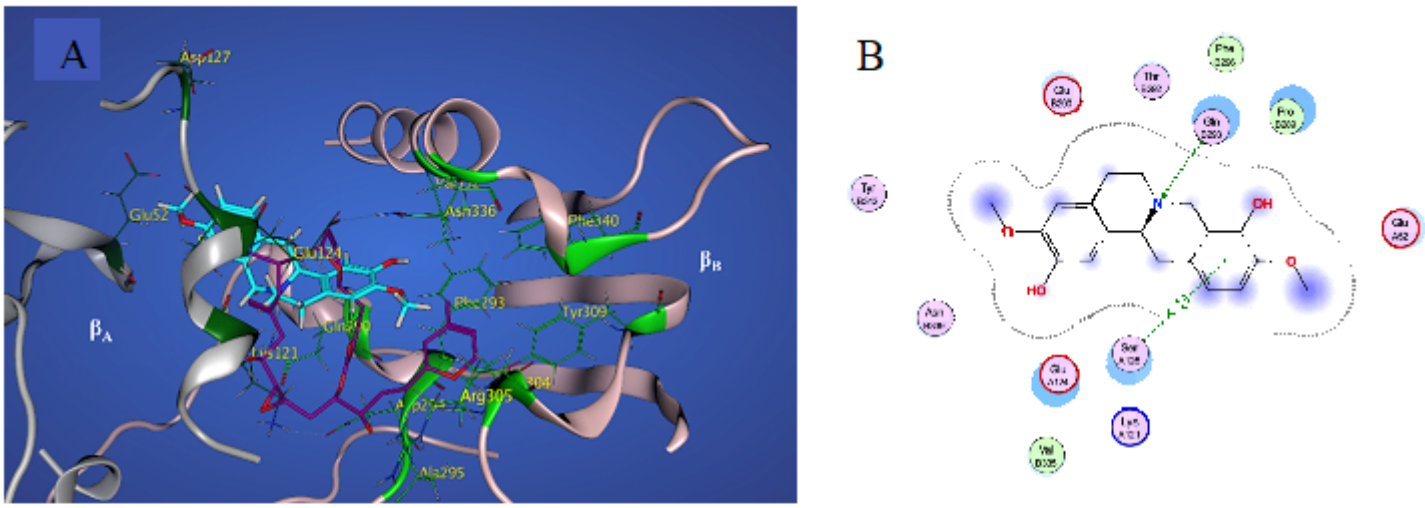


## Figure 12

A) 3D-interaction scheme of scoulerine (blue) and superimposed laulimalide crystal structure from 4O4H PDB file (purple) between microtubules. Residues in light green are in laulimalides's site on βA tubulin and residues in dark green are in laulimalides's site on βB tubulin. B) 2D-interaction scheme of Scoulerine in laulimalide binding sites on βA tubulin and βB tubulin. C) Representative structures of cluster A (purple) and cluster B (pink) in laulimalide binding sites. αA and αB tubulins colored in light and dark pink and βA and βB tubulins colored in light and dark green respectively.

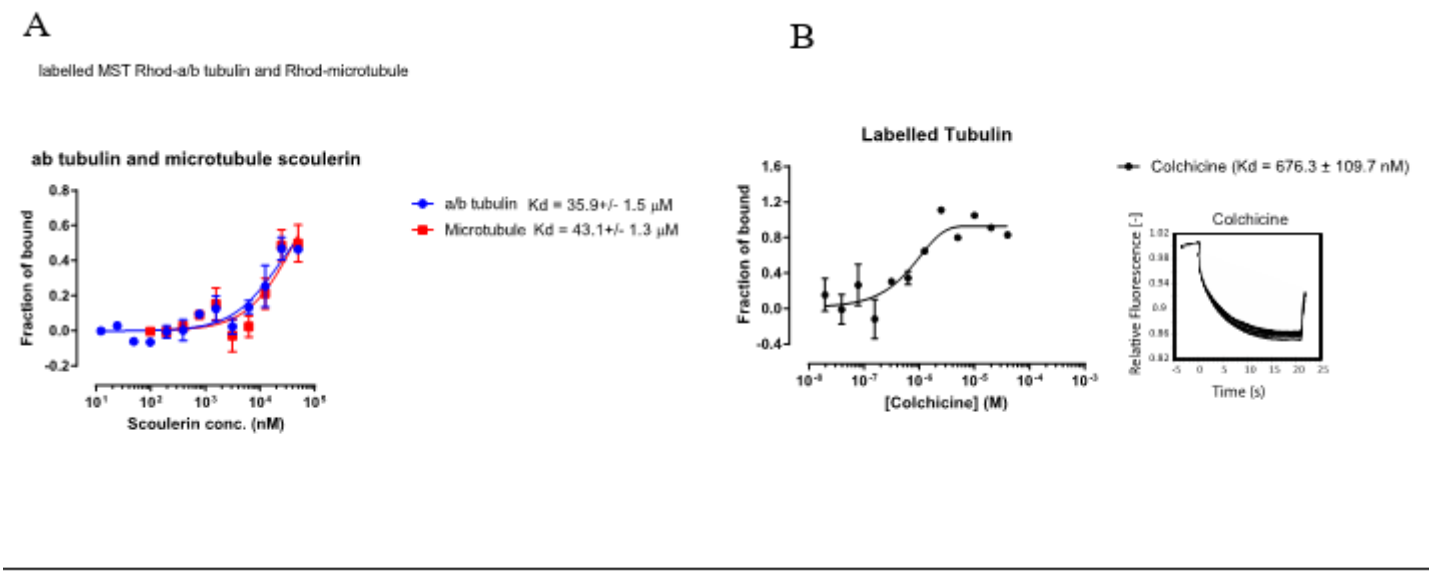


## Figure 13

A) Kd values for scoulerin bound to labelled α and β tubulin (colchicine binding site) and microtubule (laulimalide binding site) by microscale thermophoresis. B) Kd value of colchicine bound to labelled α and β tubulin (colchicine binding site) as a control.